MAY 1977

ORO SOL-
SAN 5178-77-1
UC 62

LIQUID METAL COOLED SOLAR CENTRAL RECEIVER FEASIBILITY STUDY AND HELIOSTAT FIELD ANALYSIS

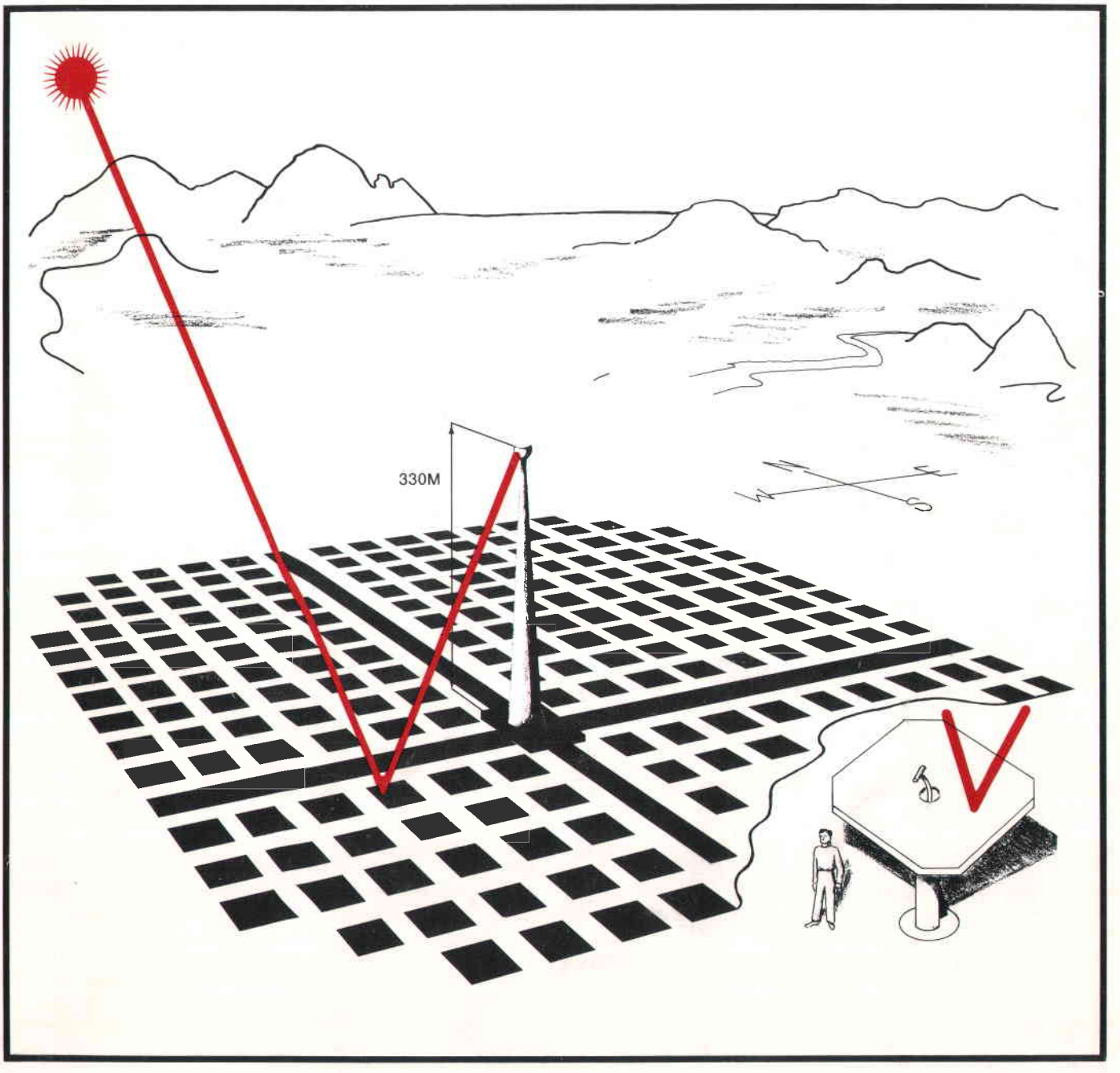

Executive Summary of Semi-Annual Review
Prepared by the
Solar Energy Laboratory, University of Houston
Under ERDA Grant No. EG-76-G-05-5178

UNIVERSITY OF HOUSTON

MCDONNELL DOUGLAS CORPORATION

Rocketdyne Division
ROCKWELL INTERNATIONAL
Atomics International Division

Printed in the United States of America
Available from
National Technical Information Service
U.S. Department of Commerce
5285 Port Royal Road
Springfield, Virginia 22161
Price: Printed Copy $4.00; Microfiche $3.00

May 1977

BIBLIOGRAPHIC DATA SHEET	1. Report No. SAN 5178-77-1	2.	3. Recipient's Accession No.

4. Title and Subtitle
Liquid Metal Cooled Solar Central Receiver
Feasibility Study and Heliostat Field Analysis

5. Report Date
5 May 1977

6.

7. Author(s)
L. Vant-Hull, G.C. Coleman, T. Springer & Co-workers

8. Performing Organization Rept. No.

9. Performing Organization Name and Address
Solar Energy Laboratory
University of Houston
Houston, Texas 77004

10. Project/Task/Work Unit No.

11. Contract/Grant No.
EG-76-G-05-5178

12. Sponsoring Organization Name and Address
Solar Energy Division
Energy Research and Development Administration
Washington, D.C.

13. Type of Report & Period Covered
Semi-Annual
6/15/76-12/15/76

14.

15. Supplementary Notes

16. Abstracts

A conceptual design for a 100 MWe Solar Tower System employing liquid sodium as a heat transfer fluid and as a storage medium is generated. This design intentionally parallels the current commercial baseline design for a water/steam transfer fluid in order to enhance comparisons between the two approaches and to maximize the application of the limited funds in this study to the unique features of the liquid sodium system. The optimization procedure to be used in the design and comparison of optimized solar tower systems at several latitudes and for variations in ground slope is described briefly. Preliminary estimates of the energy expended in constructing a solar tower system are given the initiation of an insulation data base is described.

17. Key Words and Document Analysis. 17a. Descriptors

Solar Energy
Solar Energy Concentrator
Solar Furnaces
Solar Power Generation
Solar Reflectors
Power Generators
Liquid Metal
Liquid Sodium

17b. Identifiers/Open-Ended Terms

Central Receiver
Solar Tower--Power Tower
Optical Transmission
Design Optimization
Liquid Metal
Heat Transfer

17c. COSATI Field/Group

18. Availability Statement	19. Security Class (This Report)	21. No. of Pages
NTIS	UNCLASSIFIED	33
	20. Security Class (This Page) UNCLASSIFIED	22. Price $4.00

SAN 5178-77-1
UC 62

LIQUID METAL COOLED SOLAR CENTRAL RECEIVER FEASIBILITY STUDY AND HELIOSTAT FIELD ANALYSIS

STUDY TEAM AND MANAGERS

Lorin L. Vant-Hull
Solar Energy Laboratory
UNIVERSITY OF HOUSTON

Gerry Coleman
MCDONNELL DOUGLAS ASTRONAUTICS COMPANY

Tom Springer
ATOMICS INTERNATIONAL

Jerry Friefeld
ROCKETDYNE

EXECUTIVE SUMMARY OF INFORMATION
PRESENTED AT
ERDA
SOLAR THERMAL PROJECTS SEMI-ANNUAL REVIEW
DECEMBER 7-10, 1976
DENVER, COLORADO

ABSTRACT

A conceptual design for a 100 MWe Solar Tower System employing liquid sodium as a heat transfer fluid and as a storage medium is generated. This design intentionally parallels the current commercial baseline design for a water/steam transfer fluid in order to enhance comparisons between the two approaches and to maximize the application of the limited funds in this study to the unique features of the liquid sodium system. The optimization procedure to be used in the design and comparison of optimized solar tower systems at several latitudes and for variations in ground slope is described briefly. Preliminary estimates of the energy expended in constructing a solar tower system are given and the initiation of an insolation data base is described.

TABLE OF CONTENTS

This material was prepared with the support of the U. S. Energy Research and Development Administration Grant No. EG-76-G-05-5178. However, any opinions, findings, conclusions, or recommendations expressed herein are those of the authors and do not necessarily reflect the views of ERDA.

LIST OF FIGURES

LIST OF TABLES

INTRODUCTION

In March of 1974, following the NSF semi-annual review of the solar tower feasibility studies, the NSF review board made the decision to limit further design considerations for the solar power plant to water/steam cooled receivers. At that time, liquid metal, gas, and molten salt cooled receivers were under active investigation, and all of these receivers showed promise for further development. However, it was felt the water/steam cycle represented less program risk and would be more acceptable to the utilities. Since that time, the utility-sponsored EPRI has funded the development of two gas cooled receiver concepts and Sandia has made modest advances in its molten salt receiver concept. The University of Houston, McDonnell Douglas, and Rockwell International are presently engaged in a design study of a liquid metal solar power plant.

The objectives of the liquid metal study are:

- Define the conceptual design and determine the technical feasibility of a 100 MWe sodium cooled solar central receiver system.
- Determine the preliminary cost of the liquid sodium solar energy system.
- Identify key areas requiring further technology effort.
- Evaluate latitude and ground slope effects on performance of central receiver systems.
- Determine the net energy balance for a 100 WMe water/steam solar central receiver system.

There are several advantages associated with the liquid metal cooled receiver. First, it is a low pressure system. Neither Sodium nor NaK have a significant vapor pressure at even 1000°K, well above the current peak design temperature of 867°K (1000°F). Consequently, minimum gauge tubing can be used in the receiver, reducing the wall temperature drop, thermal stress and fatigue, thermal losses, and receiver weight and cost.

Second: Liquid metals have very high thermal conductivities and do not undergo a change of state, so no surface film boiling problem exists. Consequently, temperature drops and thermal gradients are further reduced to the extent that a liquid metal cooled receiver can tolerate several times the absorbed flux allowable for a water/steam receiver.

Third: The higher flux capability significantly relaxes a constraint imposed on the water/steam receiver which requires a 50 percent larger receiver size with attendant higher thermal losses. System reoptimization without this constraint should lead to a lower cost and/or higher performance system.

Fourth: The cost of sodium is sufficiently low that one can consider storage at low or ambient pressure of the heated liquid metal. Thus, operation from storage need not differ from normal operation, improving system capacity during no sun periods (from 70 percent for 300°C oil storage) to 100 percent. The operating modes are also greatly simplified as the heated fluid from the receiver can go directly to storage and the steam generator can always operate out of storage.

Fifth: The higher conductivity and lower pressure of liquid sodium systems significantly improves overall system efficiency by permitting higher system temperatures and reheat turbines.

In addition to the liquid sodium oriented activities, the present study also continues investigations of the effects of haze, latitude and slope on the operation of the first generation central receiver water/steam system. The energy cost of materials and construction of the water/steam system is also being evaluated and compared with the energy produced over the life of the system. This type of evaluation is gaining increased recognition as our economy expends its fossil fuel reserves in producing replacement energy resources.

The liquid metal study task schedule is shown in Figure 1. System and subsystem conceptual designs have been selected and the major sodium components identified. Refined collector optimization techniques have defined the initial receiver flux and temperature profiles. The weight and energy costs of unfabricated materials required for the 10 MWe water/steam, 10 MWe pilot plant have been determined. Student evaluation of insolation data is also well underway.

FIGURE 1 **STUDY SCHEDULE**

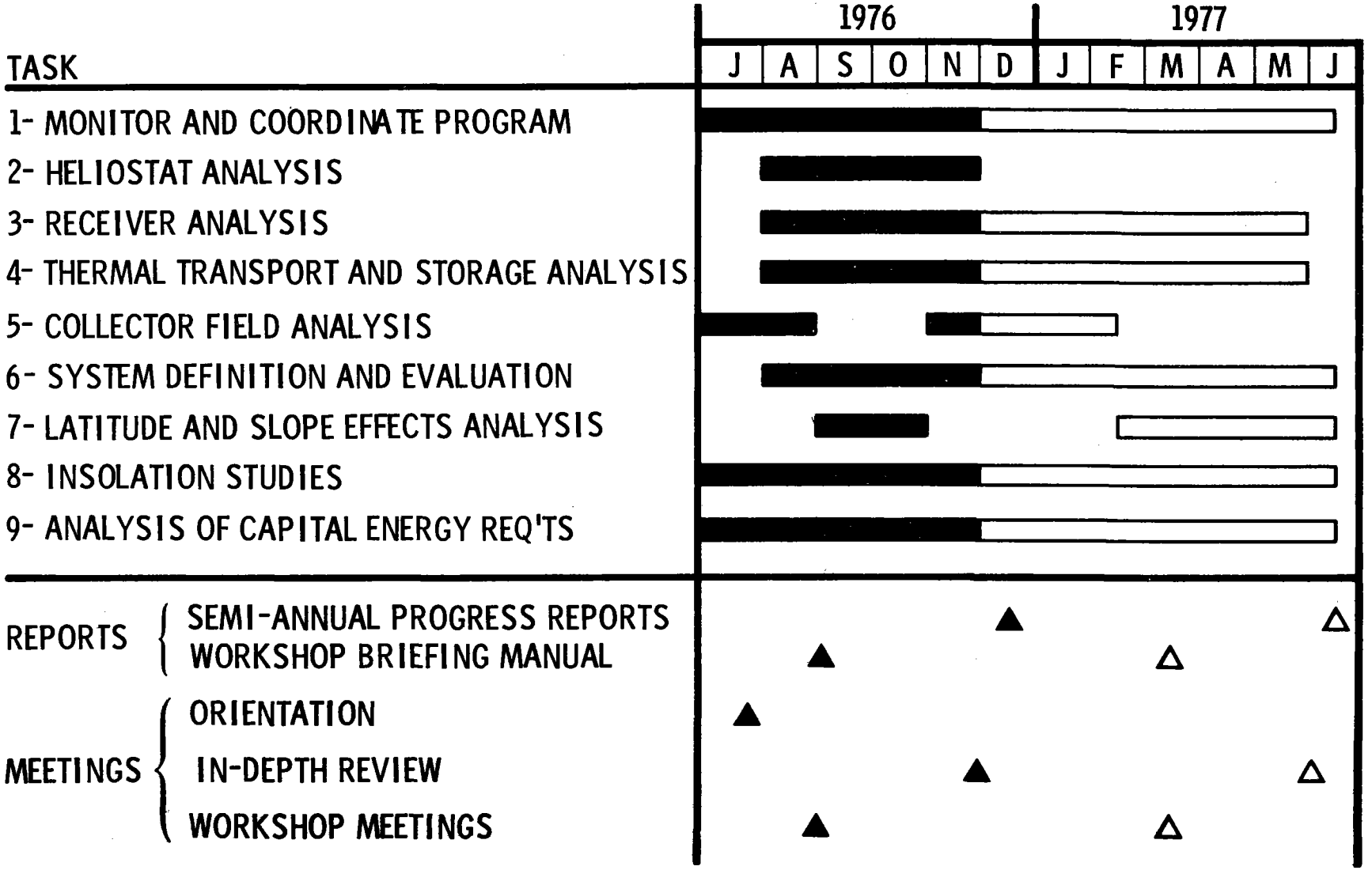

SYSTEM SUMMARY

In developing an overall description for a liquid metal system, a conscious effort has been made to duplicate as many aspects of the proposed water/steam commercial system as appears reasonable. This design duplication allows the limited funds available to be directed toward the unique aspects of the system, i.e., the liquid metal related components, and facilitates the ultimate comparison between the two system concepts.

The major requirements assumed for this study are consistent, for the most part, with the latest guidelines established for the water/steam system. A minimum plant capacity of 100 MWe net has been established as a basic requirement based on prior analysis carried out for the water/steam system, and has been assumed as the design point for the current liquid metal study. In contrast to the water/steam system which utilizes a non-reheat turbine cycle and is therefore limited to $\sim$ 100 MW capacity, the reheat cycles appropriate for the liquid metal could, in reality, reach much higher capacities. Potential economic benefits ingoing to larger capacity systems have not been included in this study due to the limited scope of the effort.

A six-hour thermal storage capacity has been specified wich allows no derating of turbine output below the 100 MWe design point. This is in contrast to the reduced power capability for the water/steam system necessary because of reduced steam temperature and pressure available from thermal storage. Although some cost penalty would result for the larger capacity liquid metal storage system, the ultimate comparison parameter of mills/KWH would reflect the corresponding increase in production of electricity.

The general nature of the receiver coolant requirement permits the evaluation of alternate liquid metal candidates which may have attractive operational features such as low freezing points. Trade studies in this area center around overall cost, performance, operational, and maintenance considerations. The balance of the requirements have been derived directly from the ongoing water/steam program.

The collector field layout appropriate for the liquid metal system, along with pertinent field related data, is shown in Figure 2. The field starts as a basic square configuration which subsequently trimmed down based on cost and performance considerations. The field is sized for an assumed solar multiple of 1.7, which was determined to be near optimum for six hours of storage based on previous water/steam system analysis. The solar multiple refers to total peak power collection capability divided by the thermal power needed to supply the turbine at its design point. This surplus power is used to charge thermal storage for the desired six hour capability. The appropriate tower structure height for this system is 213 m (700 ft) with a corresponding elevation to the receiver midpoint of 236 m (774 ft). The collector field contains 23,300 heliostats arranged in a non-uniform radial configuration. The average glass coverage fraction for the complete field is 26.3 percent.

The major system components consist of heliostats, receiver/tower, thermal storage, balance of plant, and master control. The baseline heliostat, shown in Figure 3, is an eight-segment octagonal reflector, 6.1 m (20 ft) across the flats, which uses a front surface silvered float glass with an acrylic coating. Tracking motion is produced through an elevation azimuth drive system. The receiver is an externally heated cylindrical configuration 17 m (56 ft) high by 17 m (56 ft) in diameter. It is composed of individually controlled panels which are capable of withstanding peak heat fluxes of 2 MW/m^2. The thermal storage subsystem consists of separate hot and cold tanks which contain liquid sodium, the heat exchangers, and all of the interconnecting piping and flow control equipment. A more complete description of the receiver and thermal storage subsystems is contained in subsequent sections of this summary.

The overall system schematic developed for this study is shown in Figure 4. This schematic depicts a series configuration in which all thermal power collected by the receiver first passes into the thermal storage subsystem. This is in contrast to a parallel flow configuration where thermal power flows directly from the receiver to the steam generation and reheat equipment with surplus power being shunt-fed to the thermal storage subsystem.

FIGURE 2 **COLLECTOR FIELD LAYOUT (LIQUID METAL SYSTEM)**

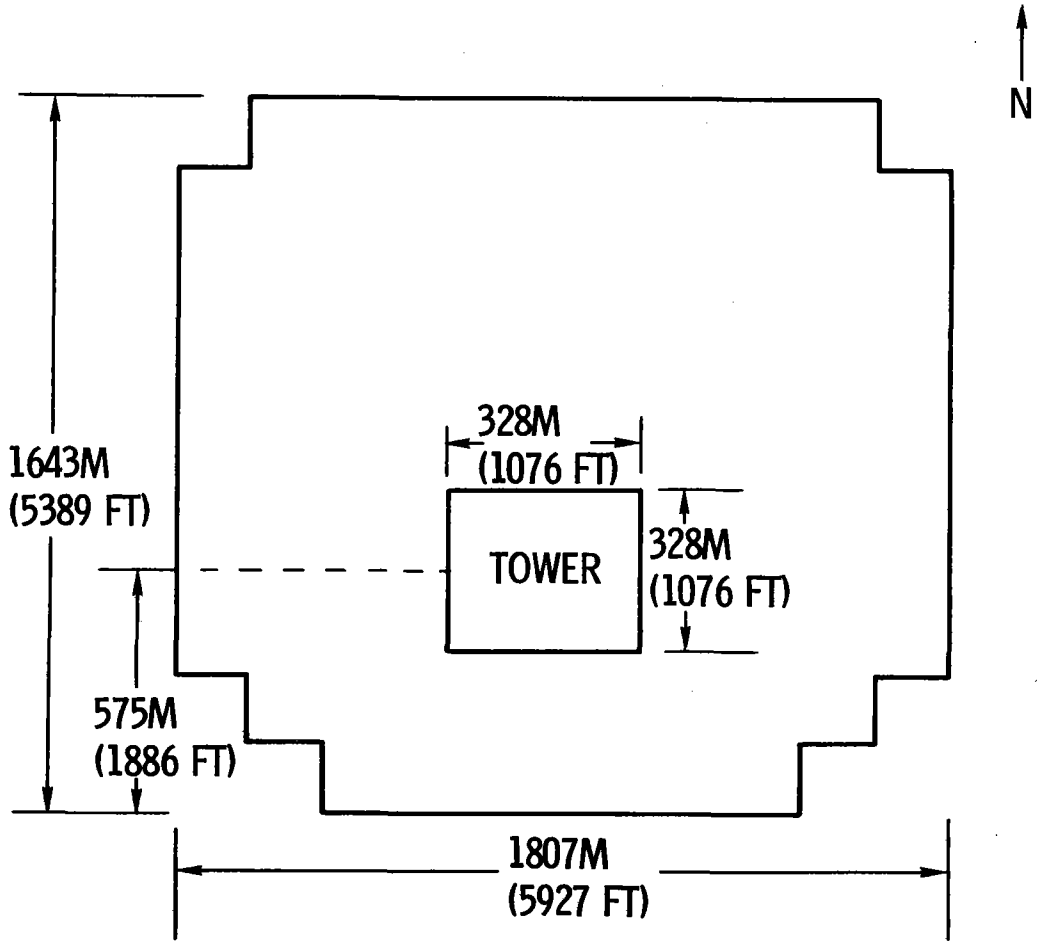

- PLANT RATING: 100 MWe NET
- SOLAR MULTIPLE: 1.70
  (6-HR EXTENDED CAPABILITY
  AT 100 MWe NET)
- RECEIVER CENTERLINE
  ELEVATION: 236M (774 FT)
- TOWER HEIGHT 213M (700 FT)
- GLASS AREA 7.14×10^5 M^2

FIGURE 3 **COLLECTOR SUBSYSTEM**

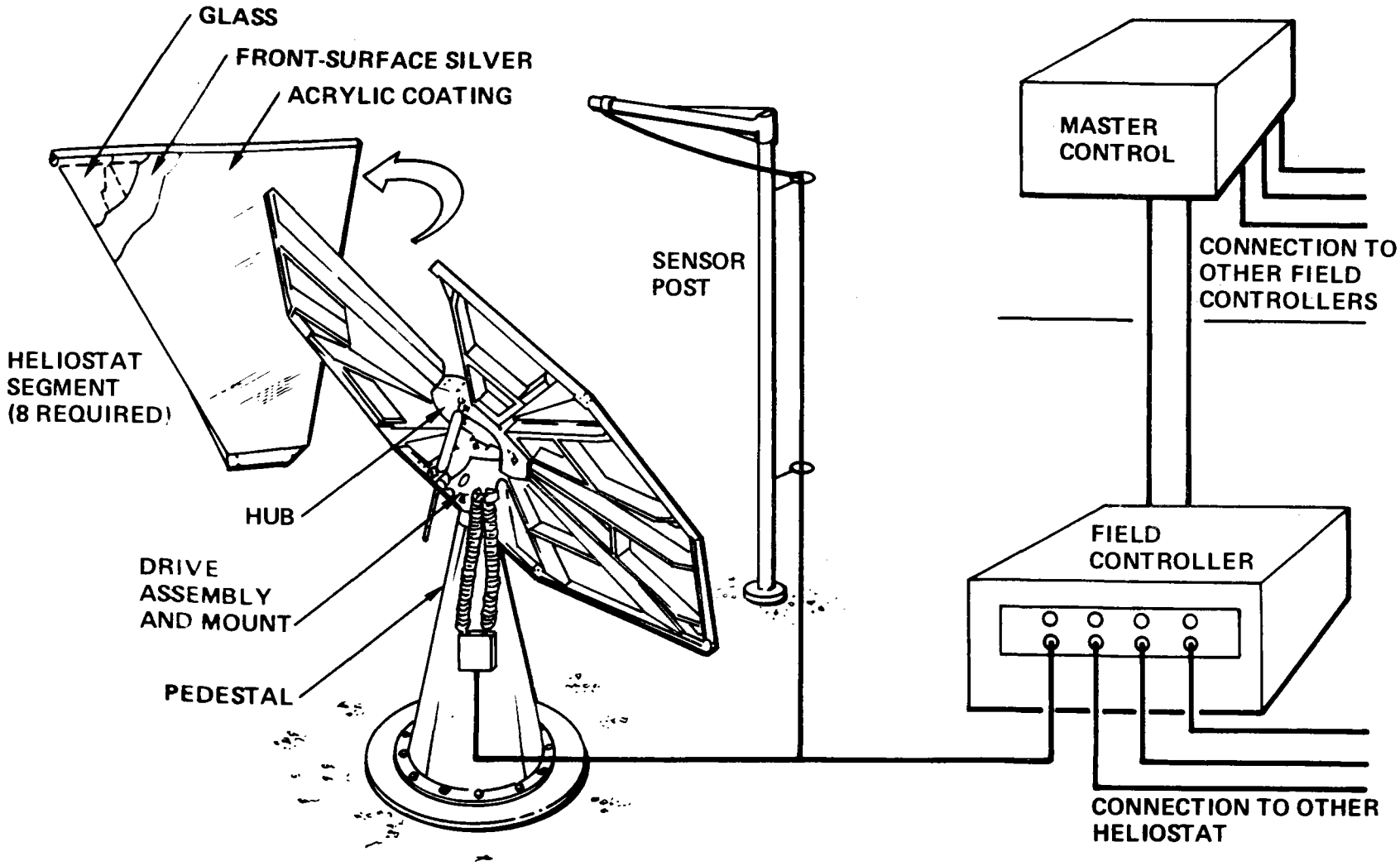

FIGURE 4 **LIQUID SODIUM SYSTEM SCHEMATIC**

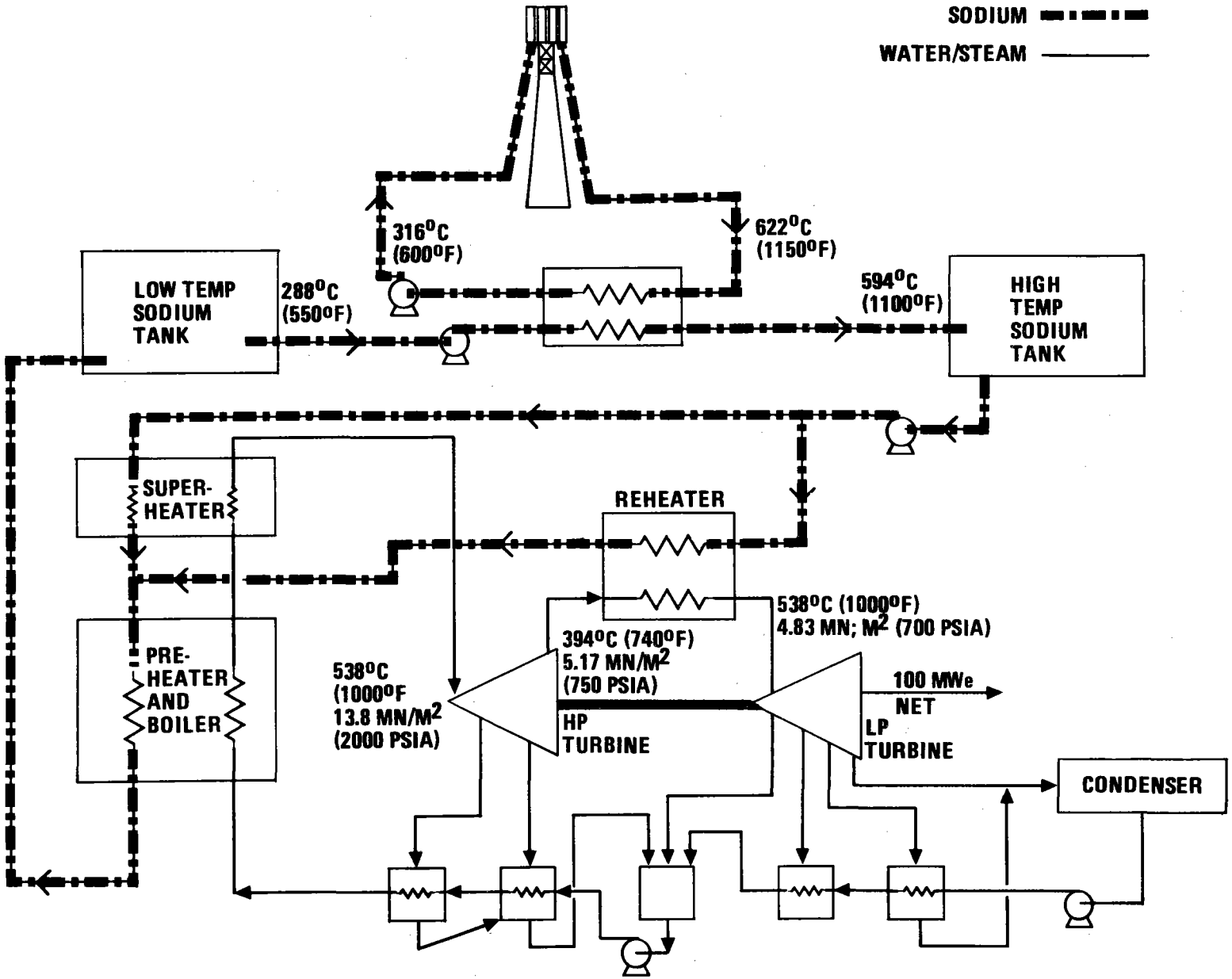

The series flow configuration, which has been selected as the baseline, has many advantages. First, the receiver loop can be decoupled from the balance of the system. This means that the complete liquid metal loops and tanks do not have to withstand the high heads which would occur at the base of a 236 m (774 ft) tall--to the receiver midpoint--tower and receiver. Also, pumping power in the receiver loop is minimized due to the pressure recovery which occurs in a closed receiver loop. Finally, the decoupling of the receiver from the turbine allows a complete buffering of the turbine from possible receiver induced transients. The major drawback to the series configuration is the requirement for an added heat exchanger at the base of the tower and the resulting need to operate the receiver at a 28°C (50°F) higher temperature.

The steam generator and reheater arrangement was selected to ensure a high temperature drop in the sodium during the steam generation and reheat operations in order to minimize fluid inventory. Restrictions related to thermal stress in the steam generator and the two-phase nature of the water/steam flow were also given consideration in establishing this baseline arrangement. The schematic also depicts the tandem compound, single reheat nature of the baseline turbine.

A high level comparison between the baseline water/steam and liquid metal systems is shown in Table 1. The table compares the cycle efficiency expected for the

two systems, anticipated annual electrical production, and resulting economic considerations. Because of the higher temperature and reheat nature of the liquid metal system cycle, a higher efficiency would be realized for that system when operating from the receiver. An even more significant disparity in efficiency occurs during periods of operation from thermal storage. Since the liquid metal system provides rated design point steam at all times, no performance penalty would occur. The water/steam system, on the other hand, experiences a significant performance penalty because of the degraded nature of the steam available from thermal storage.

TABLE 1

COMPARISON OF LIQUID METAL TO WATER/STEAM SYSTEMS

GROSS PLANT EFFICIENCY	LIQUID METAL	WATER/STEAM
• RECEIVER OPERATION	39.5%	37.6%
• THERMAL STORAGE OPERATION	39.5%	26.4%
ESTIMATED NET ANNUAL ENERGY	~ 470,000 MWHe	~ 423,000 MWHe
PERMITTED Δ COST TO PRESERVE SAME MILLS/KWHe	$14.4M	----
REDUCED COLLECTOR FIELD COSTS	~ $6.2M	----
TARGET Δ COST FOR LIQUID METAL SYSTEM	~ $20.6M	----

The impact of these efficiency characteristics on the net production of annual energy is also shown. It is seen that the liquid metal system is capable of producing ∿ 10 percent more energy on an annual basis. This means that an additional $14.4M could be spent on a liquid metal system while preserving the same value of mills/KWH . Because of higher turbine cycle and receiver efficiencies associated with the liquid metal system, additional savings of ∿$6.2M can be realized through a reduction in collector field capacity assuming Nth plant collector costs. Thus, due to smaller collector field requirements and greater electrical energy production, ∿ $20.6M could be spent on a liquid metal system above that needed for a water/steam system before a negative economic situation would result for the liquid metal system.

RECEIVER SUBSYSTEM

The overall liquid sodium heat transport arrangement, shown in Figure 5, is composed of the receiver subsystem and the thermal storage subsystem. The receiver subsystem schematic of Figure 6 contains the receiver, a pump, an expansion tank, the Modular Steam Generator (MSG) units, and the main sodium piping which includes the riser and downcomer in the tower. The steam generator units are included with the receiver subsystem on the basis that the receiver loop could be connected directly with the steam generator without the thermal storage subsystem if operation were only during hours of sunshine. The thermal storage subsystem includes only the added components necessary to provide six hours of storage operation at full power. With the flow path arrangement of Figure 5, however, direct operation of the steam generator with the receiver is not possible since all liquid sodium passes through the storage tanks. Auxiliary support to the receiver main flow loop includes the fill and drain, purification, and the inert gas and vent subsystems. Because of the static head of the sodium in the receiver and tower piping, the entire receiver loop operates at a relatively high pressure of about 2.5 MN/m^2 (350 psi). The purpose of the IHX is to isolate the static pressure due to the tower from the thermal storage tanks in order to reduce the cost of these large tanks.

The receiver subsystem sodium pump is designed for high suction pressure with developed head and flow characteristics, as shown in Figure 7. These performance characteristics are supplied by the pump currently being built for the Clinch River Breeder Reactor Program, scheduled for testing in 1979.

The main flow piping is .6 m (24-inch) O.D. with a flow velocity of about 6 m/sec (20 ft/sec.) This low flow velocity tends to minimize the system pressure loss and the pumping power required.

The receiver shown in Figure 8 is composed of 24 panels. Each panel has temperature sensors and a flow control valve for outlet temperature control.

LIQUID SODIUM HEAT TRANSPORT

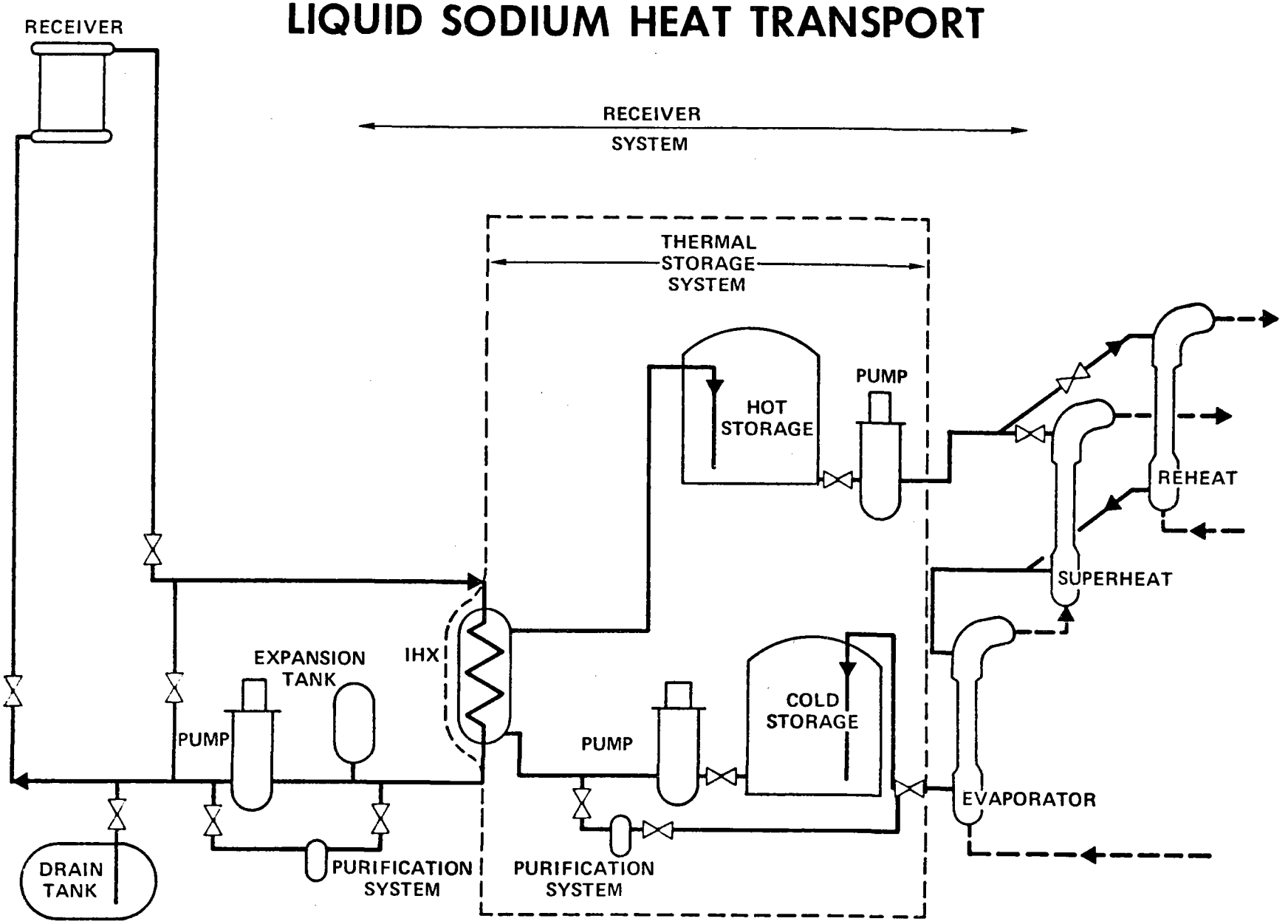

Rockwell International
Atomics International Division

FIGURE 5

76-N23-60-12

SUMMARY OF RECEIVER SODIUM LOOP BASELINE DATA

SODIUM INLET TEMPERATURE, °C (°F)	316 (600)
SODIUM OUTLET TEMPERATURE, °C (°F)	621 (1150)
MAXIMUM THERMAL POWER, MWt	506
MAXIMUM FLOW RATE, kg/h (lb/h)	4.68×10^6 (10.3×10^6)
MAXIMUM TOWER HEIGHT, M (ft)	213 (700)
SODIUM STATIC PRESSURE, MPA (psi)	2.66 (386)
MAIN PIPE OD, M (in.)	0.6 (24)

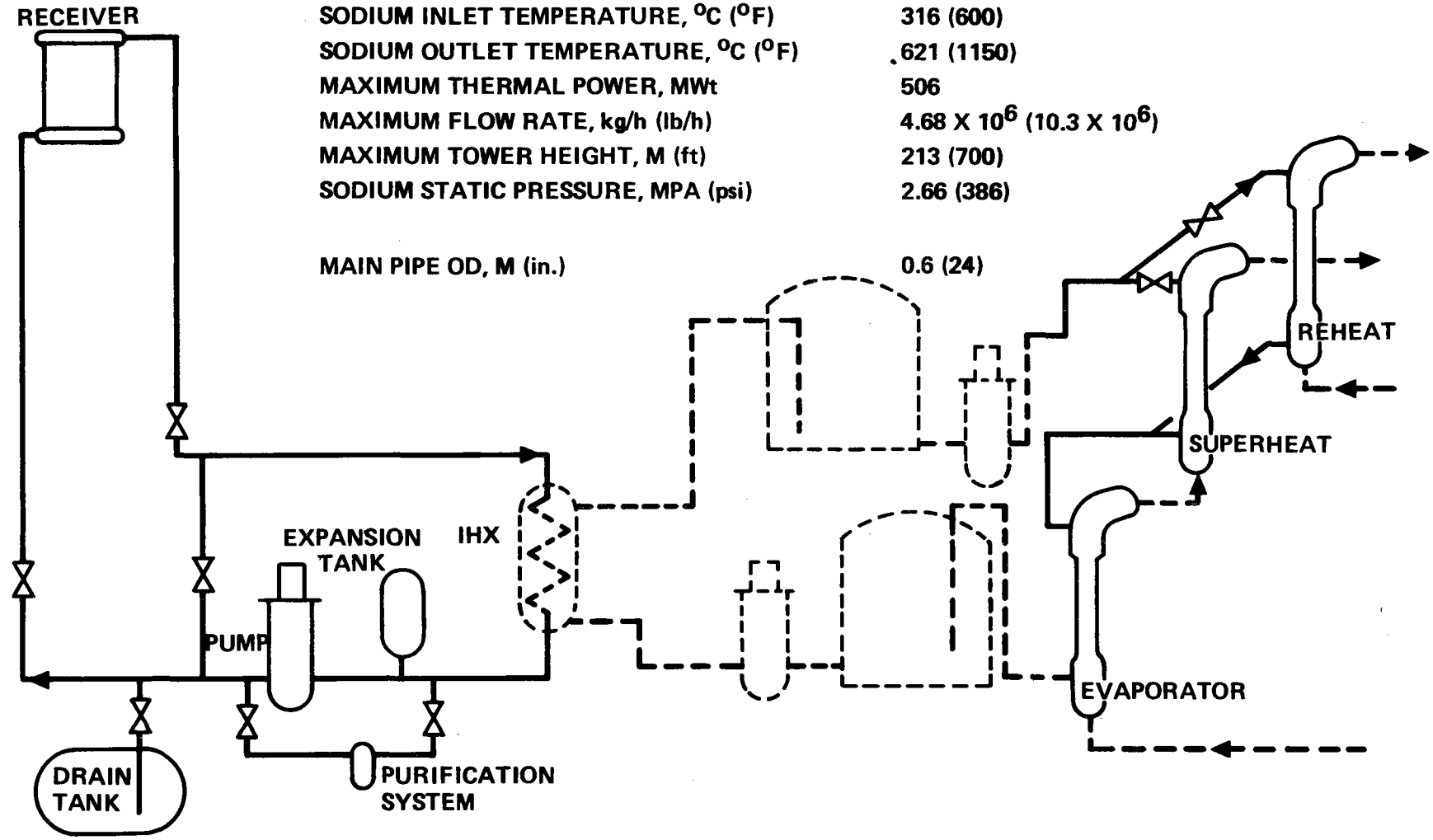

Rockwell International
Atomics International Division

FIGURE 6

FIGURE 7

SODIUM PUMPS

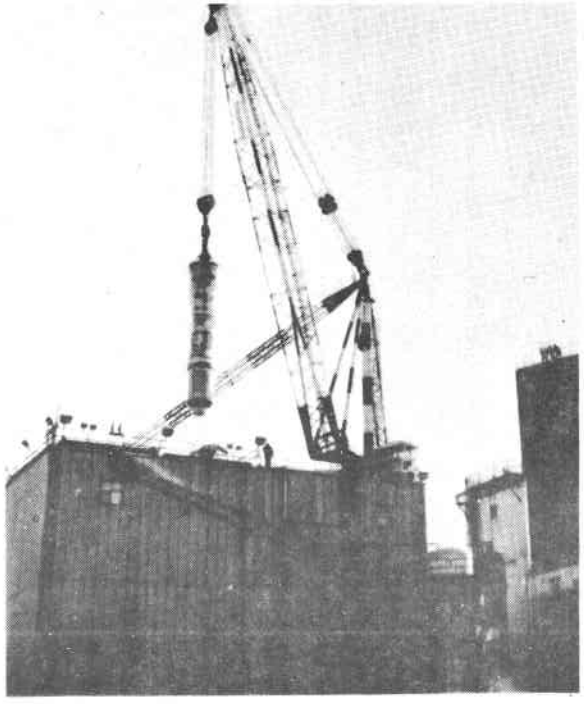

14,400 gpm SODIUM PUMP
TEST INSTALLATION AT LMEC

	STORAGE LOOP		
	RECEIVER LOOP	IHX BRANCH	STEAM GENERATOR BRANCH
FLOWRATE kg/h	4.68×10^6	4.68×10^6	2.85×10^6
(gpm)	(25,000)	(25,000)	(15,000)
DEVELOPED HEAD (M)	136	61	61
(ft)	(445)	(200)	(200)
NPSH REQUIRED (M) *	12	12	12
(ft)	(40)	(40)	(40)
MOTOR hp	4000	2000	2000

* Net Positive Suction Head

Rockwell International
Atomics International Division

FIGURE 8 **RECEIVER**

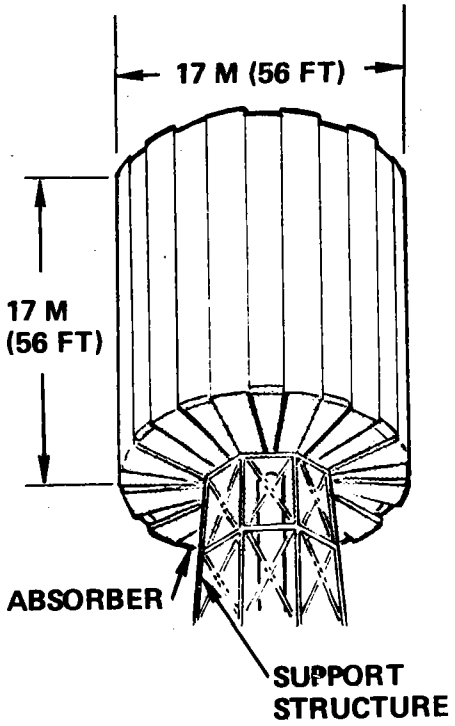

ASSEMBLY	
PEAK POWER	506 MW
PEAK FLOW, Kg/h(lb/h)	4.68×10^6 (10.3×10^6)
PRESSURE DROP, MPA (PSI)	0.2 (30 PSI)
TEMPERATURE, ^{o}C (^{o}F)	316 (600) – IN: 621 (1150) – OUT
THERMAL LOSS	9% AT PEAK POWER
	12.5 AT 50% POWER
SURFACE COATING	PYROMARK
PANELS	
NUMBER OF PANELS	24
NUMBER OF TUBES	116
WIDTH, M (FT)	2 (6.6)
PEAK HEAT FLUX, MW/M^2 (BTU/IN^2 – SEC)	1.7 (1.05)
TUBES, CM (IN)	304H STAINLESS
	1.91 (3/4) OD, 0.13 (0.05) WALL
WALL TEMPERATURE ^{o}C (^{o}F)	607 (1125) AT PEAK STRAIN POINT
	660 (1220) AT 75% OF ELEVATION

The pump is located in the cold leg of the loop. Liquid sodium is pumped to the receiver at a temperature of 316°C (600°F) and leaves the receiver at 622°C (1150°F).

A receiver bypass line and valve permit odium circulation without passing through the receiver, which may facilitate the daily startup and shutdown operation.

The steam generating equipment is an arrangement of ten modular units. Four units function as evaporator, four units for superheat, and two units for reheat. The superheat and reheat units are constructed of stainless steel for high temperature operation. The evaporator units are constructed of 2-1/4 Cr - 1 Mo. The Modular Steam Generator, pictured in Figure 9, is manufactured by Atomics International. A unit was successfully tested with liquid sodium in 1972 and 1973 for over 9000 hours.

FIGURE 9

STEAM GENERATOR

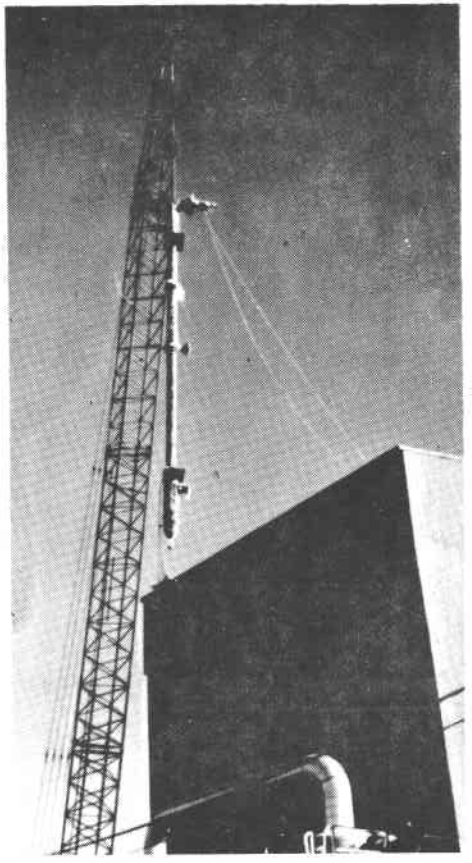

MODULAR STEAM GENERATOR
TEST INSTALLATION AT
LMEC

	SODIUM	WATER/ STEAM
• STEAM GENERATOR TEMPERATURE IN, °C	593	205
(°F)	(1100)	(400)
• STEAM GENERATOR TEMPERATURE OUT, °C	288	538
(°F)	(550)	(1000)
• MAXIMUM THERMAL POWER, MWt	→ 305 ←	
• MAXIMUM FLOW RATE, kg/h	2.85×10^6	3.92×10^5
(lb/h)	(6.28×10^6)	(8.6×10^5)

• STEAM GENERATOR

	EVAPORATORS	SUPER-HEATER	REHEAT
MSG UNITS	4	4	2
TUBE SIZE, OD M	0.0158	0.0158	
(in.)	(5/8)	(5/8)	
NO. OF TUBES	158	158	
HEAT TRANSFER AREA, M^2	140	140	
(ft^2)	(1500)	(1500)	
TUBE MATERIAL	2-1/4 Cr – 1 Mo	304H SS	

Rockwell International
Atomics International Division

THERMAL STORAGE SUBSYSTEMS

The thermal storage subsystem, shown in Figure 10, contains the hot and cold storage liquid sodium tanks, two pumps, and the Intermediate Heat Exchanger (IHX). Liquid sodium from the IHX is stored in the hot storage tank at energy rates up to 506 MWt, which corresponds to a flow rate of 1300 Kgm/sec (10.3×10^6 lb/hr.) Sodium is drawn from the hot storage tank at energy rates of up to 305 MWt or 786 Kgm/sec (6.28×10^6 lb/hr) to generate steam for the Electric Power Generating Subsystem. Sodium from the MSG units flows to the cold storage tank. During the day, hot sodium is accumulated by the hot tank in a sufficient quantity to store up to six hours of operation at 100 percent rated power. With this storage arrangement, plant operation is always from storage. The steam conditions provided are the same regardless of whether the receiver loop is operating or not.

Two pumps are required in this subsystem to move the liquid sodium between the hot and cold storage tanks. The cold leg pump must have a flow capacity of 1300 Kgm/sec (10.3×10 lb/hr) to accomplish the charging operation through the IHX to the hot storage tank. This pump is similar to the CRBRP pump used in the receiver subsystem, Figure 7, but with reduced developed head requirements. The hot leg pump with a flow capacity of 786 Kgm/sec (6.28×10^6 lb/hr) moves the liquid sodium through the steam generators to the cold tank. This pump is also similar to the CRBRP pump of Figure 7, with both reduced head and flow requirements. The developed head requirements for these pumps will be moderate - on the order of 60 m (200 feet). The pumps will be located below the storage tank elevation so that adequate suction head is available even when the liquid level in the tanks is low. The liquid sodium pump being developed for the Clinch River Breeder Reactor Program is suitable for these two applications.

The sodium-to-sodium IHX, with characteristics as shown in Figure 11, is arranged so that the tube side flow is part of the high pressure receiver loop and the shell side flow is part of the thermal storage system. The IHX may be based on the unit being built for CRBRP, with tube bundle lengthened to obtain the capability for 506 MWt power.

FIGURE 10

SUMMARY OF THERMAL STORAGE LOOP BASELINE SYSTEM

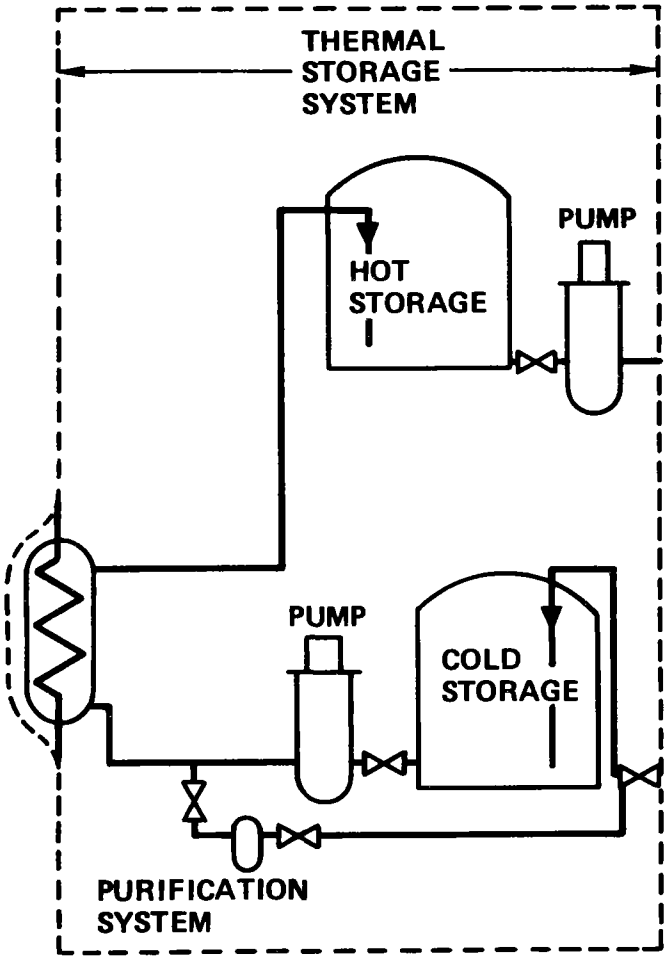

ENERGY IN STORAGE, MWt-h	1830	
TEMPERATURE: HOT LEG, °C (°F)	593	(1100)
COLD LEG, °C (°F)	288	(550)
WEIGHT OF SODIUM, kg (lb)	1.7×10^7	(3.76×10^7)
VOLUME OF SODIUM, M^3 (gal)	20120	(5.3×10^6)
STORAGE TANK SIZE, M (ft)	38ϕ X 19	$(125\phi$ X 63)

	IHX BRANCH	SG BRANCH
FLOWRATE: kg/h (lb/h)	4.7×10^6 (10.3×10^6)	2.85×10^6 (6.28×10^6)
THERMAL POWER, MWt	506 (MAX)	305

FIGURE 11

INTERMEDIATE HEAT EXCHANGER (IHX)

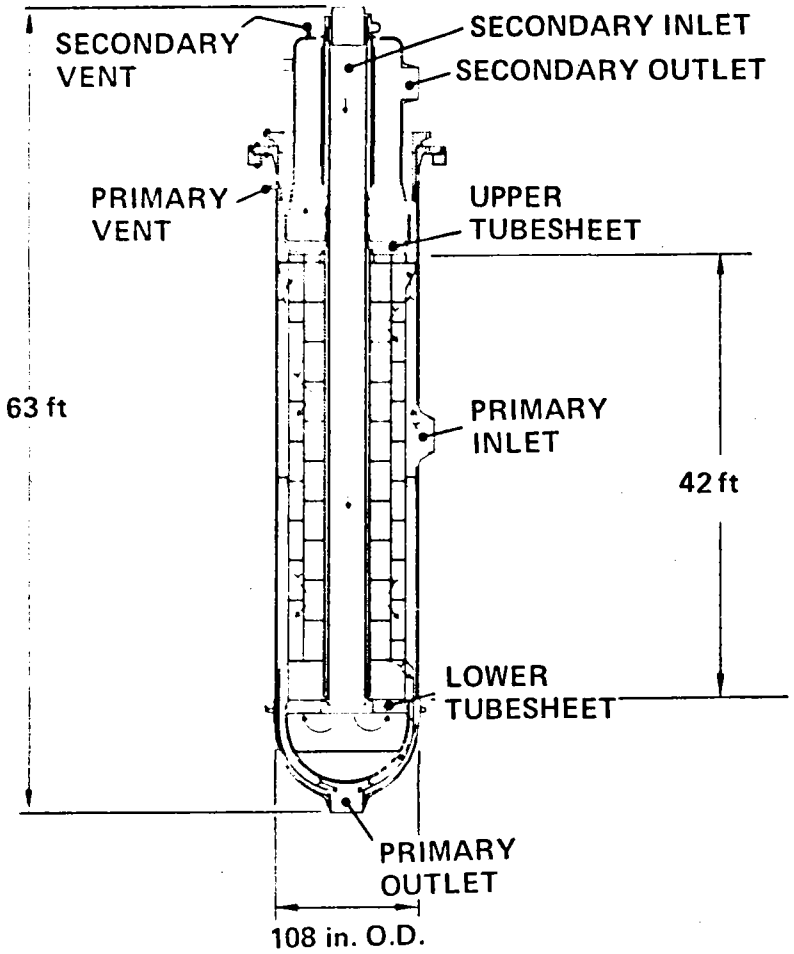

• THERMAL POWER, (MWt)	506
• PRIMARY FLOW, kg/h (lb/h)	4.68 X 10^6 (10.3 X 10^6)
• PRIMARY INLET TEMPERATURE, °C (°F)	622 (1150)
• LMTD, °C (°F)	28 (50)
• TUBE O.D., M (in.)	0.0158 (5/8)
• MATERIAL	SS
• HEAT TRANSFER SURFACE, M^2 (ft^2)	1915 (20600)
• NUMBER OF TUBES	2,770
• PRESSURE LOSS: PRIMARY, MPA (psi)	0.10 (15)
SECONDARY, MPA (psi)	0.08 (12)

COLLECTOR FIELD DESIGN

Introduction

In the solar tower system, subject to a few basic design decisions, the design of the solar receiver and the design of the heliostats are essentially independent. The overall system is integrated through the collector field design in which the locations of the individual heliostats and the perimeter of the heliostat field are specified. Given this information, the optical properties of the heliostats and the position of the sun define the flux pattern and its temporal variation on the receiver. Within certain limits an "aiming strategy" can be used to redistribute the flux to reduce the peak flux, but care must be exercised or excessive beam spillage may occur.

In our current design work, we assume an external, cylindrical tube-wall receiver in which the concentrated solar heat is absorbed into a working fluid. Such a receiver places the minimum restrictions on the extent of the heliostat field. With the exception of a relatively small exclusion region of about 30° on the axis of the cylinder (in which the generating plant can be located) the heliostats view a receiver which is not significantly foreshortened by angle of incidence effects.

In contrast, if a cavity receiver were used, heliostats far off the normal to the plane of the aperture would see a foreshortened aperture; at 60° off normal, the aperture appears as an ellipse with minor axis half the true diameter of the aperture. This effect either forces an increase in the aperture diameter (with increased losses approaching those of the equivalent cylinder) or restricts the angular size of the heliostat field. If a given energy level is specified, this angular restriction will lead to the requirement for a taller tower and, due to divergence of the solar beam, a larger aperture.

For large scale systems, the advantages of focussing heliostats becomes negligible. For a 100 MWe system slant ranges of over 1 km prevail for the more distant heliostats, and a typical beam error is σ = 3 mrad. Perfectly

Table 2. Peak Absorbed Flux and Interception Factors for Several Cylindrical Receivers

QUANTITY		PEAK FLUX		INTERCEPTION	
AIM STRATEGY		belt*	hi-lo**	belt*	hi-lo**
DIAMETER	LENGTH				
17 m	17 m	1.75	1.50	.966	.951
15 m	17 m	2.0	1.63	.952	.937
15 m	15 m	2.0	--	--	.937

belt* - Each heliostat is aimed at the near point on the equator of the cylindrical receiver.

hi-lo**- The aim point of alternate heliostats is shifted up (down) so the edge of the beam grazes the top (bottom) of the receiver.

focussed heliostats would produce a 15 m (50 ft) diameter image, while the effective diameter of the image from a 6 m (20 ft) diameter flat heliostat at the same range would be about 16 m (53 ft). Trial calculations have verified that there is no significant increase in concentration accruing to focussed heliostats at this scale. Consequently, computationally and mechanically simpler flat heliostats are chosen as baseline for these studies. In contrast, for smaller systems (such as the 10 MWe pilot plant) a certain degree of focussing is required to produce an effective simulation of the larger scale system. As a consequence of these considerations, the cylindrical external receiver has been chosen for use with flat (non-focussing) heliostats for our general field optimization routines.

Collector for Liquid-Metal System

Preliminary analysis indicated that the liquid sodium receiver would operate in the temperature range 550°C to 650°C ($\sim$ 1000°F to 1200°F) and at a peak flux up to about 2.0 MW/m^2 (1.2 BTU/in^2-sec). These conditions are known to be reasonable and attainable for an external receiver. From prior ERDA contracts, detailed design approaches and computer routines were available for the heat transfer and thermal fatigue calculations for an external tube-sheet cylindrical receiver. In addition, preliminary heliostat field configurations and heliostat array optimization routines for this configuration were available. Consequently, to make maximum use of the limited time and funding available, and to allow easy comparison with the MDAC water-steam baseline design, a similar external receiver configuration was chosen.

Using a preliminary 100 MWe collector field, receiver flux profiles were generated for flat and canted segment (partially focussing) baseline heliostats. Using these results, we selected a receiver 17 m (56 ft) in diameter and 17 m (56 ft) high as a preliminary baseline for the sodium-cooled receiver study. The aberrations associated with partially focussing heliostats lead to more complex problems in the form of time-dependent receiver flux profiles and interception factors, as well as somewhat more peaked receiver fluxes. As no clear advantage

resulted from focussing, we chose to baseline the flat heliostat.

Price estimates for the liquid-metal receiver and the associated pumps and heat exchangers were not available early in the study. Rather than design a field based on fictitious costs, we chose to use the collector field design from the currently ongoing water/steam receiver study. It was felt that the receiver/tower subsystem cost would be reasonably comparable in the two cases. Consequently, in the second quarter, receiver flux profiles and interception factors were generated for this collector field and the baseline receiver. For system trade purposes, several other cases were also investigated with results shown in Table 2. Annual data (consisting of outputs hourly on the 21st of each month) for the panel power and gradients was also generated for the 17 x 17 m receiver for each aim strategy. After a more detailed receiver study, system analysis, and cost estimation, it is anticipated that a new baseline field specifically designed to optimize the performance of a liquid-sodium system may be required in the last quarter of this study. If, for example, costs associated with the sodium receiver were substantially higher than comparable costs for a steam receiver, a larger collector field would be required to minimize system cost per KW or per KWhr.

Latitude and Slope Study

The effects of latitude and slope on the performance of a solar tower system have not previously been investigated in any consistent manner. This would be a simple matter if, for example, the performance of a uniform collector with a 30% ground coverage factor and a central tower was computed at different latitudes and for different ground slopes. However, it is necessary to optimize the heliostat array, ground coverage, and extent of the field for each location in order to compare the "best" system for each case.

For this work to be valid, it is necessary to have a well-defined performance and cost model. Consequently, we will use the 100 MWe external water/steam receiver and other components currently defined by the McDonnell Douglas team as commercial baseline for their work in the 10 MWe Pilot Plant Design Study.

This receiver is 17 m (56 ft) in diameter, 25.5 m (84 ft) high. The current peak flux limitation of 0.6 MWth/m^2 (.37 BTU/in^2-sec) absorbed onto the receiver is subject to results of subsystem research experiments currently in progress. Because this limitation would complicate the design procedure and can be overcome by modification in aiming strategy and modest receiver redesigns, it will be ignored in this work. For this receiver we will design comparable fields optimized at 0° slope and 25° N, 35° N, and 45° N, latitude and at 10° and 15° slope (up to north) at 35° latitude. In addition, a nonsymmetric field with improved afternoon performance will be designed for 0° slope, 35° N latitude operation.

The procedure used to optimize the heliostat locations and the field perimeter is based on a rather lengthy analysis, which will be released as a separate publication. There are two new programs used in the optimization, which may be iterated. In this discussion we will assume experience, or a prior iteration, can provide a reasonable idea of the required tower height and field size to deliver the required thermal power to the specified receiver. For the baseline requirements at 35°N latitude, this suggests, as a preliminary input, a focal length (vertical distance from plane of heliostat centers to center line of receiver), h, of 232 m (760 ft) and an 11 x 11 field of cells each h/2 on a side. We consider the performance of a reference heliostat at the center of each cell.

As a first step, we compute loss footprints (Figure 12) giving, for each azimuth, the separation required for a single neighbor to yield a specific shading and blocking loss, i.e. 1, 2 or 4%. This routine is extremely fast because the overlapping of multiple events is ignored. Consequently, a good sample of times can be used. We use 19 times equally spaced (or concentrated at lower elevations where shading and blocking is significant) between the operational solar elevations of ± 15° on each of seven typical days (monthly, starting at the summer solstice). Using these footprints, we determine the most effective heliostat configuration in each cell, for example, that configuration giving maximum ground coverage with a total annual loss of ∿ 6% due to all neighboring

Figure 12.

HELIOSTAT LOSS FOOTPRINTS
ANNUAL SHADING AND BLOCKING LOSS

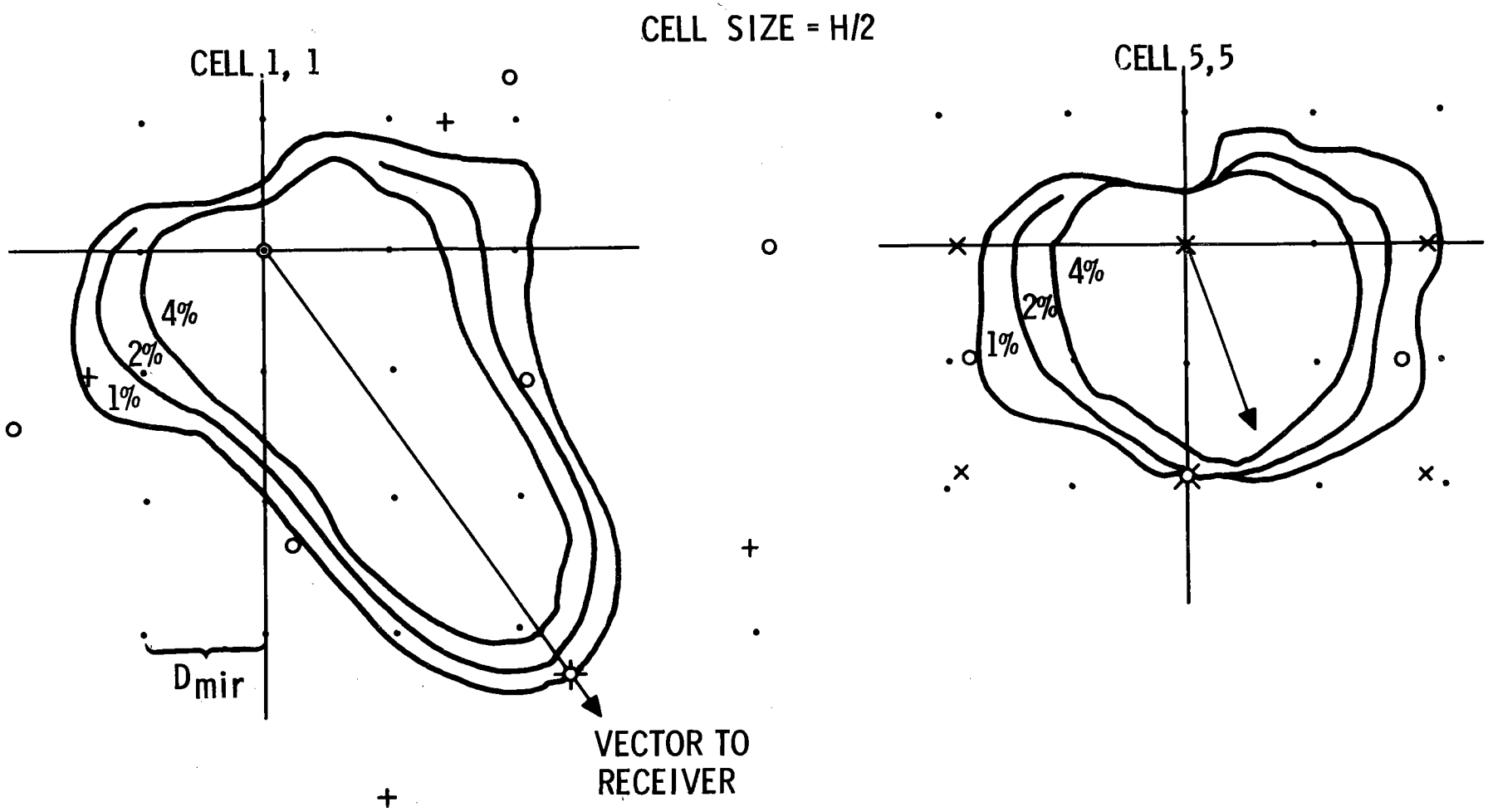

LOCATION OF NEIGHBORS

- o RADIAL STAGGER
- × RADIAL ORTHOGONAL

LOCATION OF NEIGHBORS

- o N - S STAGGER
- × NORTH-SOUTH
  EAST-WEST

heliostats. In general, a radially oriented, staggered field tends to give the best performance, although we routinely compare radial and north-south orientation of simple rectangular and of staggered (face centered) arrays. Having chosen the configuration, we must still determine the optimum spacing. The computer routine used to generate input data (receiver interception factors and preliminary heliostat spacings in each cell) for our optimization routine is indicated in Figure 13. We wish to place as many heliostats as possible in each cell without excessively degrading their performance. However, the performance depends upon the following factors, each of which is computed for the representative heliostat at the center of each cell: 1) the insolation-weighted aperture of the heliostat (essentially $\int\sigma \cos i \, dt / \int\sigma \, dt$, 2) the shading and blocking loss, 3) the total loss suffered by all other heliostats in a cell due to crowding one additional heliostat into the cell, 4) the cost per heliostat of land, site preparation, and wiring the heliostats to the field controllers, and 5) the fraction of redirected energy intercepted by the specified receiver. All these factors as well as the ratio of the total cost of the thermal system to the heliostat cost are considered in defining the heliostat spacing in each cell. The computer procedures leading to definition of the optimum spacings are shown in Figure 14.

In practice, the Lagrangian energy per square meter of reflector (the net increase in energy from the cell due to adding one square meter of reflector) at the desired operating point is specified for each cell, and an interpolation routine searches for the intersection of that line with the line of maximum redirected energy for a given ground coverage. After the operating point is defined in each cell, a trim routine (Figure 15) orders the cells based on receiver energy per dollar (including wiring and land costs which become excessive in the sparsely populated periphery of the field). Thermal system cost and the received power from each cell are summed, taking account of all optical or thermal losses, and the optimum is defined as that array of cells giving minimum cost in (dollars) $(\text{MWhr/year})^{-1}$. For a typical case, the cost of the various subsystems in the thermal collection component of an early 100 MWe commercial central receiver system is as follows: the heliostat field (72.6%), cabling for heliostat control and power (7.8%), receiver (7.4%), riser, downcomer and control valves (3.6%), Tower (4.2%), and land and site preparation (4.4%). The cost of the thermal storage unit is not considered in our current

Figure 13.

DATA FLOW SCHEMATIC FOR CELL-WISE OPTIMIZATION PROCEDURE

(DATA ARE ENCLOSED BY PARENTHESES)

TO GENERATE THE "PANEL" DATA FILE

(INPUT)	INPUT PROGRAM CONTAINS HELIOSTAT DESIGN, ETC.
↓	
YRN2	MAIN PROGRAM INCLUDES SHADING AND BLOCKING
↓	
HCOEF	IMAGE GENERATOR
↓	
CYLN	RECEIVER PROGRAM
↓	
(PANEL)	OUTPUT DATA FILE CONTAINS PANEL INTERCEPTION FACTORS.

TO GENERATE AN INITIAL HELIOSTAT ARRAY

LOSS	OUTPUTS CONTOURS OF LOST ENERGY VERSUS COORDINATES OF A NEIGHBORING HELIOSTAT.
↓	
(ACELL1)	CONTAINS 4 OPTIONAL CHOICES FOR X_1 AND X_2 SPACING PARAMETERS IN EACH CELL.
↓	
FGRND	OUTPUTS GROUND COVERAGE MATRIX (FGRND) FOR ALL 4 OPTIONS AND SELECTS OPTION MAXIMIZING FGRND IN EACH CELL SUBJECT TO MECHANICAL CONSTRAINTS.
↓	
(ACELL2)	CONTAINS BEST CHOICE FOR X_1 AND X_2 FOR EACH CELL

Figure 14.

DATA FLOW SCHEMATIC FOR CELL-WISE OPTIMIZATION PROCEDURE - (CONTINUED)

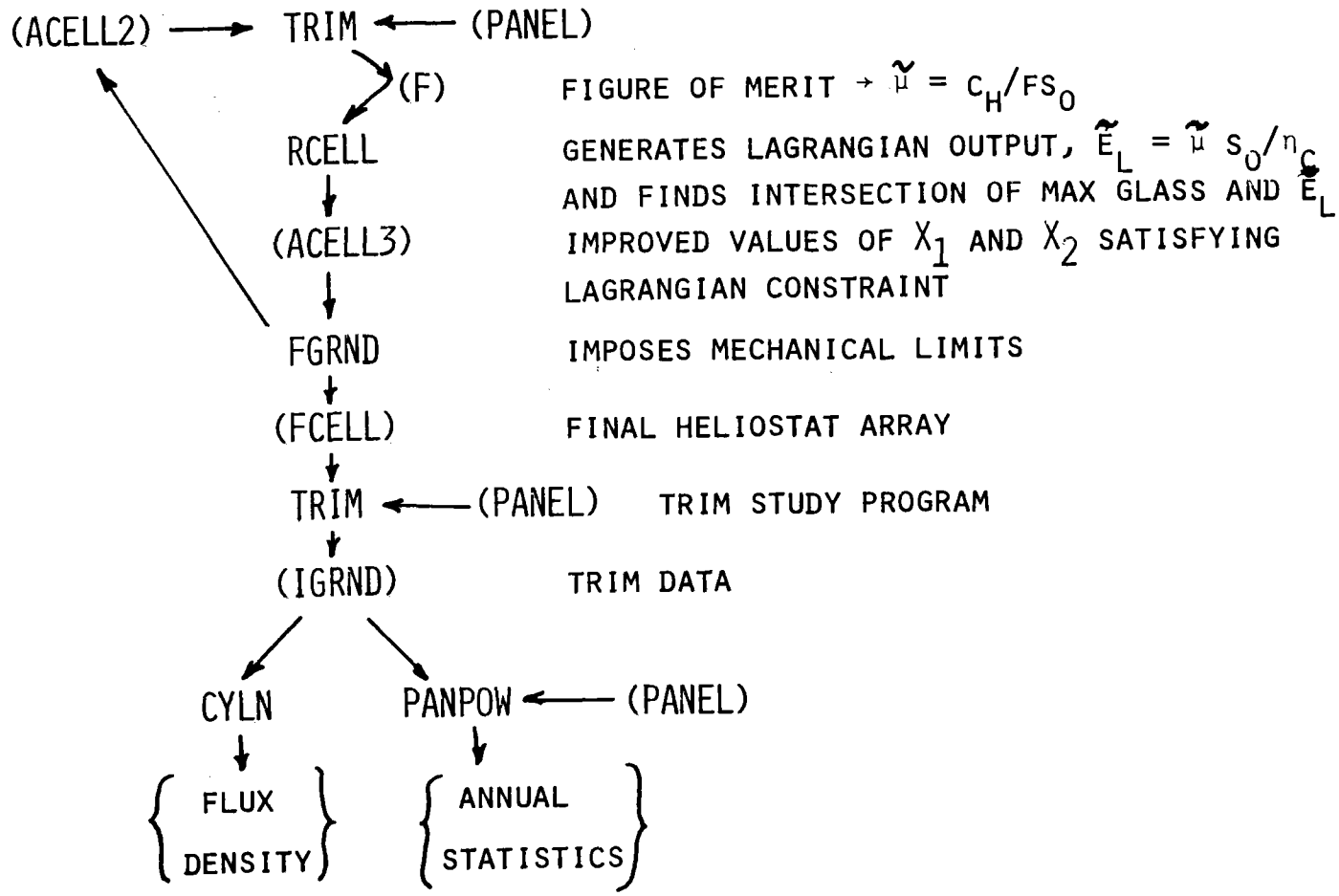

Figure 15.

T R I M R O U T I N E

- o READS HELIOSTAT LOCATIONS AND INTERCEPTION FACTORS
- o GENERATES ANNUAL SHADING, BLOCKING AND COSINE I DATA
- o ADJUSTS MIRROR PERFORMANCE FOR LAND AND WIRING COSTS
- o ORDERS CELLS BASED ON ADJUSTED PERFORMANCE
- o COMPUTES AND PRINTS FOR EACH ADDED CELL
  - . ANNUAL CELL PERFORMANCE IN MWH_R/M^2 - YEAR
  - . TOTAL RECEIVER ENERGY/YEAR IN MWH_R
  - . FIGURE OF MERIT FOR COLLECTOR F $\Rightarrow$ $\mu = C/F$
  - . NET RECEIVER POWER AND NET PANEL POWERS ON GIVEN HOUR
  - . FRACTIONAL COST BY COMPONENT AND TOTAL COLLECTOR COST
- o REPEATS FOR DESIRED ADJUSTMENT IN TYPE OR NUMBER OF RECEIVER PANELS

analysis, although the thermal energy in excess of the turbogenerator requirement will be stored. We currently consider the size and cost of this system as subject to an overall system trade study. By combing these sub-system costs with the corresponding annual collected energy, a figure of merit is calculated, which is used as input to a further convergent iteration leading finally to a definition of the optimum configuration.

The optimum field is subject to certain restrictions. Examples include guaranteeing free rotation of heliostats, providing adequate access to the mirrors for cleaning and servicing, and receiver peak flux and gradient limitations.

Finally the power available at the design point, e.g. 10 a.m. and 2 p.m. on equinox day, is computed and compared to the system requirement. This would typically include a provision for filling storage expressed through a solar multiple, i.e. the ratio (peak power)/(power required to operate the turbine at rated capacity). A typical solar multiple is 1.7, which along with a requirement for 100 MWe net output, typical parasitic loads of 12 MWe, and a turbine efficiency of 37.6% gives a requirement for 506 MWth deposited in the downcoming receiver steam. If the power available is not 506 MWth, the collector field size, number of heliostats, and the tower height would be scaled to provide the correct power. At this correct scale, and remaining cognizant of the various restrictions just mentioned, the optimization will be iterated, if needed, to achieve the final optimum field, and diurnal and annual performance will be computed, cost per KWe installed and per KWhr delivered will be estimated, etc., all on a compatible basis for the several latitudes and slopes involved in the study.

In all this work, symmetry between the east and west portions of the field is assumed because the solar position is symmetric about local solar noon. If one assumes a premium is placed on afternoon power to match an assumed demand curve which peaks in the late afternoon and that only minimal storage is available for system stability requirements, this diurnal symmetry is broken, and a field design favoring afternoon energy collection will result. By designing such a field under an otherwise consistent set of assumptions, the value of this approach can be evaluated.

INSOLATION MODELING

Reliable data for direct beam insolation are very sparse. To date we have concentrated on locating this data in computer compatible formats, for we are not equipped to digitize strip chart data. After all available data are collected, a set of reasonably cloud free days will be chosen. For these we will attempt to achieve reasonable correlations between insolation, air mass, and the various meterological measurements, such as visibility, precipitable water or humidity, turbidity, etc. Eventually, we hope to achieve a relatively simple functional relationship suitable as input for our computer routines. We are currently using such a model, but it lacks detailed confirmation.

NET ENERGY

The ratio of the energy output of an energy producing system to the energy required to reproduce that system may be defined as an Energy Amplification Factor, EAF. This number has recently been defined in ERDA 76-1 for a nuclear power plant including the initial fuel charge as 3.85. In Table 3, we show results of a preliminary study which includes only the processing of raw materials for a pilot plant. We must yet evaluate fabrication and transportation energy and the conversion from thermal energy at a remote site to the appropriate energy form needed. We must also add the cost of some small components and carry out correct scaling to a commercial system. From our preliminary result, it seems likely that the total thermal energy required can be produced in one year. Assuming a net conversion efficiency of 33%, three years are required to reproduce a facility within 30 years design life, leading to an preliminary estimated EAF of $\simeq$ 10 for the Solar Tower. This work will be refined and a detailed analysis presented in the final report.

Table 3. PRELIMINARY ESTIMATE OF THERMAL COLLECTION COMPONENT -- $10MW_E$ PILOT PLANT (2000 HELIOSTATS)

PART	MATERIAL(1)	WEIGHT(1) (Kg)	ENERGY REQUIRED IN KWH_t
HELIOSTAT (ONE)	GLASS	487.16	1.58×10^3 (2)
	STEEL	903.8	6.79×10^3 (3)
	CONCRETE	8546	8.55×10^3 (4)
		SUM (one)	1.692×10^4
HELIOSTATS (2K)			TOTAL (2K) 3.384×10^7
RECEIVER	INCOLOY 800 (STEEL)	4.36×10^4	3.24×10^5 (3)
RISER AND DOWNCOMER	STEEL	8.48×10^3	6.30×10^4 (3)
TOWER			
STEEL	CONCRETE	1.341×10^6	1.34×10^6 (4)
	STEEL	2.34×10^5	1.738×10^6 (3)
			TOTAL 3.08×10^6
CONCRETE	CONCRETE	6.57×10^6	6.57×10^6 (4)
	STEEL	2.88×10^5	2.14×10^6 (3)
			TOTAL 8.71×10^6

SYSTEM	TOTAL ENERGY REQUIRED IN KWH_t	DAYS TO PROVIDE THERMAL EQUIVALENT FROM RECEIVER
2K HELIOSTATS & STEEL TOWER	3.73×10^7	150
2K HELIOSTATS & CONCRETE TOWER	4.29×10^7	173

REFERENCES

(1) McDonnell Douglas Astronautics Company, Central Receiver Solar Thermal Power System, MDC G6040, MDC 6063, MDC G6318, MDC G 6349, MDC G6382 and C. R. Applebaugh, personal communication.

(2) Cszesney and Bigley (Guardian Industries), personal communication.

(3) E. Hirst, Mech Eng 96, #9, 32 (Sept. 1974).

(4) J. Kistemaker, "Energie-Analyse von de Total Kernenergie Cyclas Gebaseerd op Licht Water Reactoren," Assoc. Eusatom - FOM, Zomer 1975, p. 10, Table 2.